

Effect of Welding Variables on Lamellar Tearing Susceptibility in the Lehigh Test

Energy required to cause failure after welding is found to disclose some additional aspects of lamellar tearing that are not indicated by the critical weld restraint level (CWRL)

BY S. GANESH AND R. D. STOUT

ABSTRACT. The effect of welding variables on lamellar tearing susceptibility was studied with the Lehigh lamellar tearing test. This provided a quantitative measure of susceptibility under controlled laboratory conditions.

Initially, the critical weld restraint level (CWRL) required to cause failure of the joint was employed as an index of lamellar tearing susceptibility. This parameter (CWRL) was observed to be unresponsive to large increases in the heat input, despite significant changes in the fracture features as evidenced by an increase in the proportion of ductile lamellar tears to brittle cleavage. This suggested that CWRL may not be the most sensitive criterion of tearing susceptibility and a more appropriate index might be the strain required to induce a critical level of tearing in the joint.

The Lehigh test was, therefore, instrumented to record the joint displacement and load during the testing process. The energy required to cause failure after the joint was welded, called the postweld energy index, was employed as a criterion to assess the extent of damage through lamellar tearing. The postweld energy index was shown to increase with an increase in heat input, preheat and with the use of an alternately reversed weld-pass direction.

The improvement with high heat input and preheat was associated with the interception and blunting of pre-existing tears by the finger penetration of the overlying weld. In the presence of hydrogen, the tearing susceptibility showed a significant increase and frac-

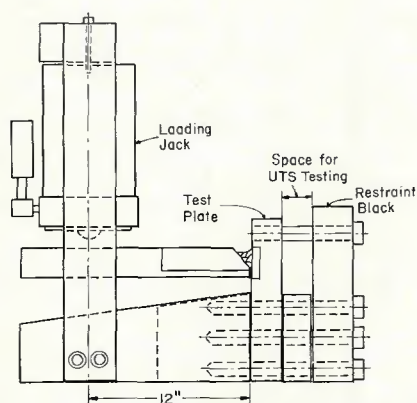


Fig. 1—Lehigh lamellar tearing fixture

ture occurred by a combination of microvoid coalescence and quasi-cleavage.

Introduction

In a welded joint, lamellar tearing results from a combination of high through-thickness strain and poor short-transverse ductility. While the overall weldment strain depends on the amount of joint contraction and the restraint intensity of the surrounding structure, the local stress-strain distributions are highly heterogeneous as a result of the complex interaction of weld thermal gradients and the constraint imposed by the surrounding continuum. The through-thickness ductility is governed by metallurgical

variables such as type, size, shape and spacing of non-metallic inclusions, matrix structure, banding, and embrittling mechanisms that may act during (or after) welding to lower the local ductility.

In a susceptible material, the incidence of lamellar tearing may be minimized, if not eliminated, by a judicious selection of welding conditions and pass sequence. However, there are conflicting reports in the literature regarding the effect of welding variables on the lamellar tearing susceptibility. For instance, while pre-heat and maintenance of high inter-pass temperature is reported (Refs. 1-5) to improve lamellar tearing resistance, it has also been found (Refs. 6, 7) to produce the reverse effect, depending on how the preheat is applied.

It is generally agreed (Refs. 2, 8) that, for a given joint size, the tearing tendency decreases with an increase in the heat input. According to some Japanese investigators (Refs. 5, 9, 10) lamellar tearing is a form of delayed cracking displaying a decreasing tendency to tearing with a decrease in the diffusible hydrogen of the weld; while according to some British investigators (Refs. 2, 3), it is a moderately elevated temperature phenomenon occurring in the temperature range 200–300 C (392–572 F).

These contradictions may be attributed, in part, to lack of quantitative data on the tearing susceptibility and to dissimilarity in the weldability tests employed by the various investigators. To probe this situation, a quantitative weldability test was developed (Ref. 1)

S. GANESH is with Bendix Research Laboratories, Southfield, Michigan, and R. D. STOUT is Dean, Graduate School, Lehigh University, Bethlehem, Pennsylvania.

at Lehigh to study the effect of material and welding variables on lamellar tearing susceptibility.

The Lehigh test (Fig. 1) employs a cantilever beam joined to a rigid vertical test plate with a multi-pass weld in a 45 deg bevel groove under a constant level of through-thickness stress applied by externally loading the cantilever. The external load is increased proportionally to the cross sectional area of the weld, after each weld layer has cooled to the interpass temperature, to maintain the desired level of through-thickness stress (called the weld restraint level).

Different specimens taken from the same material are tested at various levels of weld restraint. The level just necessary to cause failure of the joint during testing, without the need for an overload is considered the critical weld restraint level (CWRL) and represents the lamellar tearing susceptibility of that material. By this criterion the tearing susceptibility of a wide range of steels was determined and related to inclusion type and distribution, oxygen content, microstructural features and fracture mechanisms in these steels.

The results from that study were presented in an earlier paper (Ref. 11). From among the materials tested, three steels—one semi-killed, one silicon-killed and one aluminum-killed—were chosen to study the effect of welding conditions on the lamellar tearing susceptibility. The compositions of the test steels are given in Table 1 and their microstructural and fracture characteristics, in Table 2.

Study Using the Stress Criterion (CWRL)

The semi-killed A-285C (M) plate having displayed a low resistance to lamellar tearing, was chosen to study the effect of welding variables on the tearing susceptibility. Also the tears in this material were observed to initiate within the heat-affected zone (HAZ) and, hence, might be expected to be susceptible to the influence of hydrogen and heat input variations. The heat input was varied by changing the travel speed while maintaining the current and voltage constant. The additional heat inputs chosen were 30 kJ/in. (12 kJ/cm), 90 kJ/in. (35 kJ/cm), and 160 kJ/in. (63 kJ/cm) requiring 13, 5 and 3 passes respectively to fill the joint. The welding conditions employed are presented in Table 3 and the pass sequence is illustrated in Fig. 2.

In earlier tests, a high-strength low-alloy steel wire, A-632, was used as the filler metal to confine the plastic strains to the test plate. But, as this wire was no longer available in the

market, a second wire, AX110, with slightly different chemistry and properties, was chosen as a substitute. To check if a lower strength weld metal would have any effect on the susceptibility, a mild steel wire, A-675, having a considerably lower strength than the AX110 (Table 3) was used as a filler metal to evaluate the susceptibility of the A-285 steel. The effect of 120 C (248 F) preheat was studied with the AX110 wire at 45 kJ/in. (1772 kJ/m) and 160 kJ/in. (63 kJ/cm).

As tear initiation tended to be located near the weld finish side of the plate, tests were conducted in which the direction of welding was alternately reversed to check for any improvement in the tearing susceptibility.

Results

The test results on semi-killed A-285 (M) steel under different welding conditions are presented in Table 4; the observed variations in susceptibility, as indicated by the CWRL, are summarized in Table 5. It can be seen that despite a large (3 to 1) variation in the heat input, no significant difference (<8%) in the CWRL was

observed. Also, practically no change was evident with the three filler metals employed, despite a large difference in their strength levels. This likely resulted from the fact that they were all overmatched to the base metal. Alternating the welding direction did not produce any improvement in the CWRL; but failure initiated at the left side of the specimen in one test and at the right, in the other. Preheating was more effective, producing about 10% rise in CWRL at 45 kJ/in. (18 kJ/cm) and 30% rise at 160 kJ/in. (63 kJ/cm).

Failure occurred by ductile lamellar tear initiation and cleavage propagation, the proportion of which varied with the heat input as shown in Fig. 3. When the load imposed was greater than the CWRL, failure occurred during welding while the material was still hot. Metallographic examination of specimens tested below CWRL showed the tearing to initiate in the HAZ, both at low and high heat inputs—Fig. 4.

At low heat inputs, little tearing was found outside the main crack front, whereas at the high heat inputs, arrays of subcritical tears were observed to lie along the HAZ—Fig. 5.

Table 1—Composition of Test Steels

Material Thickness, mm Code Deoxidation practice	A-285C 32 M Semi- killed	A-515-70 25 F Silicon- killed	MIL-24113C 25 U Aluminum- killed
C	0.22%	0.25%	0.15%
Mn	.41	.73	1.24
P	.002	.005	.011
S	.027	.024	.019
Si	.06	.28	.29
Ni	.12	.02	.20
Cr	.06	.02	.17
Cu	.25	.052	.086
Al	<.005	<.005	.047
Sn	.007	<.002	.002
N	.0050	.0047	.0064
O	.0090	.0042	.0069
Ce	—	.006	—

Table 2—Summary of Observations on Test Steels

Material	A-285C	A-515-70	MIL 24113C
Matrix structure	Randomly orientated (ferrite + pearlite, grain size = 3)	Elongated (ferrite + pearlite, grain size = 3)	Severely banded (ferrite + pearlite, grain size = 7)
Inclusion type:			
Major	Silicates	Silicates	Type III MnS
Minor	Type I MnS (Fe, Mn) O	Type I MnS (Fe, Mn) O	Alumina, Type I MnS
CWRL ksi (MPa)	53 (365)	61 (420)	58 (400)
Location of tears	Lower HAZ	Below HAZ	Below HAZ
Fracture mode:			
Initiation	Lamellar tearing	Lamellar tearing	Lamellar tearing
Propagation	Cleavage	Cleavage	Lamellar tearing

Table 3—Welding Conditions and Filler Metals

Procedure code	Filler metal ^(a) type	No. passes	No. of layers	Interpass temperature C	Heat input		Current, A	Voltage, V	Travel speed	
					kJ/in.	(kJ/m)			ipm	(mm/s)
A	A-632	9	4	R.T.	45	(1772)	310	28.5	12	(5.1)
B	A-632	5	3	R.T.	90	(3543)	310	28.5	6	(2.5)
C	A-632	13	5	R.T.	30	(1181)	310	28.5	18	(7.6)
D	AX110	9	4	R.T.	45	(1772)	310	28.5	12	(5.1)
E	AX110	5	3	R.T.	90	(3543)	310	28.5	6	(2.5)
F	AX110	13	5	R.T.	30	(1181)	310	28.5	18	(7.6)
G	A-675	9	4	R.T.	45	(1772)	310	28.5	12	(5.1)
H	AX110	9	4	120	45	(1772)	310	28.5	12	(5.1)
I ^(b)	AX110	9	4	R.T.	45	(1772)	310	28.5	12	(5.1)
J	AX110	3	2	R.T.	160	(6300)	430	32.0	5	(2.1)
K	AX110	3	2	120	160	(6300)	430	32.0	5	(2.1)
L ^(c)	AX110	9	4	R.T.	45	(1772)	310	28.5	12	(5.1)

Composition, %

No.	Filler metal	C	Mn	Si	Al	S	P	Mo	Ni	Cr	V	Ti
1	A-632	.07	1.35	.50	—	.012	.010	.45	1.30	—	.15	—
2	AX110	.08	1.70	.46	.003	.009	.005	.50	2.40	.05	.02	.025
3	A-675	.11	1.09	.52	—	.024	.016	—	—	—	—	—

Mechanical properties^(d)

	Filler metal	UTS		YS,		Elong., RA		C _v n	
		ksi	(MPa)	ksi	(MPa)	%	%	at -50 C (-58 F),	(Nm)
1	A-632	123	(848)	109	(752)	22	65	70	(96)
2	AX110	134	(924)	125	(862)	20.5	66	59	(81)
3	A-675	84	(579)	68	(469)	32	69	35	(48)

(a) All filler metals were 0.045 in. (1.14 mm) in diameter.

(b) Alternate weld direction.

(c) Hydrogen.

(d) UTS—ultimate tensile strength; YS—yield strength; Elong.—elongation; RA—reduction in area; C_vn—Charpy V-notch.

Thus, although the CWRL was insensitive to large variations in the welding heat input, the fracture surface showed significant changes in the proportion of ductile lamellar tears to brittle cleavage.

Discussion

As pointed out in an earlier paper

(Ref. 11), tearing in the Lehigh test tended to initiate during welding in the end portion of the weld, adjacent to the toe of the preceding layer. This was possibly due to a transient overload resulting from the reduction in the effective section supporting the external load as the molten puddle entered the junction of start tab and

test plate, expanding and weakening that area.

The magnitude of overload was a function of the applied load and the ratio of the volume of the molten puddle to the volume of the weldment. The volume of the molten puddle increased with an increase in the heat input and preheat and, consequently, the overload increased as well. Also, with an increase in the heat input and preheat, the temperature in the end portion during overload was higher.

These conditions were conducive to initiating lamellar tears, and the greater proportion of ductile tears observed at higher heat input and preheat was understandable. The variation in fracture mode suggested that the amount of strain involved in the tearing process might vary significantly with changes in the welding conditions, despite the lack of change in the critical weld restraint level.

It was felt that a more informative criterion for tearing susceptibility might be the energy required for failure since this incorporates the effects of both strength and ductility. Hence, in subsequent tests, an energy criterion was used to evaluate the lamellar tearing susceptibility under various welding conditions.

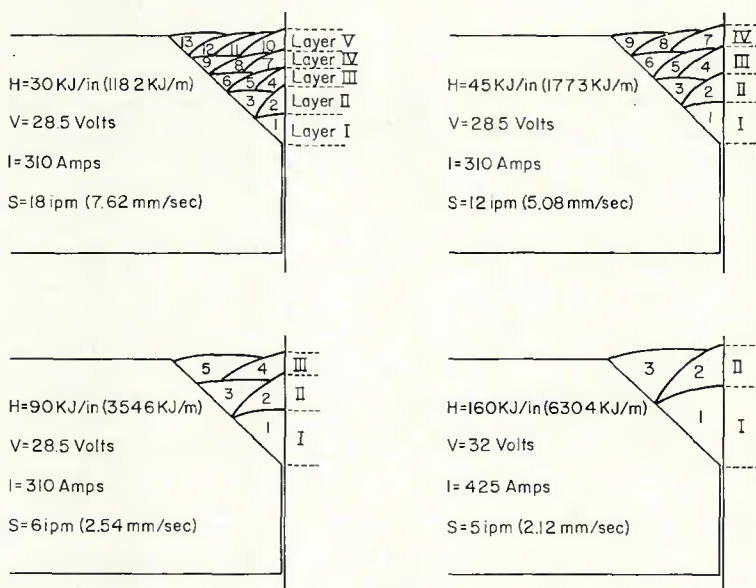


Fig. 2—Welding sequence under different conditions

Table 4—Test Results on Semi-Killed A-285 Using the Stress Criterion (CWRL)

Welding condition	Filler metal	WRL, ksi (MPa)	Failure	Fracture stress,		Remarks	CWRL, ksi (MPa)
				ksi	(MPa)		
30 kJ/in. (12 kJ/cm)	A-632	46 (317)	No	51	(393)	—	Failed about ½ h after loading
		50 (345)	No	51	(352)	51 (352)	
		52 (359)	Yes	—	—	—	
45 kJ/in. (18 kJ/cm)	A-632	48 (331)	No	—	—	Examined metallographically	53 (365)
		52 (359)	No	53	(365)	—	
		56 (386)	Yes	—	—	Failed while loading after 6th pass	
	AX110	60 (414)	Yes	—	—	Failed while loading after 6th pass	51 (352)
		50 (345)	No	50.5	(348)	Failed about 3 h after loading	
		54 (372)	Yes	—	—	Failed while loading after 9th pass	
		A-675	50 (345)	No	51	(352)	
54 (372)	Yes		—	—	Failed while loading after 9th pass		
90 kJ/in. (35 kJ/cm)	A-632	52 (359)	No	59	(407)	—	54 (372)
		56 (386)	Yes	—	—	Failed during 5th pass	
		60 (414)	Yes	—	—	Failed while loading after 3rd pass	
	AX110	46 (317)	No	—	—	Examined metallographically	51 (352)
		50 (345)	No	51	(352)	—	
		54 (372)	Yes	—	—	Failed during 5th pass	
45 kJ/in. (18 kJ/cm) + Preheat 120 C	AX110	52 (359)	No	60	(414)	—	55 (379)
		56 (386)	Yes	—	—	Failed during 8th pass	
		62 (427)	Yes	—	—	Failed during 9th pass	
45 kJ/in. (18 kJ/cm) Alternate weld direction	AX110	50 (345)	No	55	(379)	Failure initiated at left-hand side	52 (359)
		54 (372)	Yes	—	—	Failure initiated at the right-hand side during 8th pass	
160 kJ/in. (63 kJ/cm) + Preheat 120 C	AX110	50 (345)	No	57	(392)	—	65 (450)
		60 (414)	No	65	(450)	—	
		65 (450)	Yes	63	(435)	Failed on loading after final pass	

Table 5—Effect of Welding Conditions on the Tearing Susceptibility (CWRL) of Semi-Killed A-285 (M)—1¼ in.

Welding condition	Filler metal		
	A-632	AX110	A-675
45 kJ/in. (18 kJ/cm)	53 (365)	51 (352)	52 (359)
45 kJ/in. ^(a) (18 kJ/cm)	—	55 (379)	—
45 kJ/in. ^(b) (18 kJ/cm)	—	52 (359)	—
30 kJ/in. (12 kJ/cm)	51 (352)	—	—
90 kJ/in. (35 kJ/cm)	54 (372)	51 (352)	—
160 kJ/in. ^(a) (63 kJ/cm)	—	65 (450)	—

(a) Plus 120 C preheat (b) Alternate weld direction

Study Using the Energy Criterion

The Lehigh test was instrumented to enable the recording of load and joint displacement so that the energy required for failure could be evaluated under different conditions. The set up is shown in Fig. 6. For recording the load, a load cell was placed between the hydraulic jack and the cantilever. The relative displacement between the test plate and the cantilever was recorded by a clip gage mounted between two rigid extensions taken from fixed points on the test plate and the cantilever. With this arrangement, the electrode holder could pass through the joint without interfering with the clip gage; hence, the



Fig. 3—Fracture appearance at (a) low and (b) high heat input in semi-killed A-285 steel

displacement could be recorded continuously during the test process. The extensions were attached on the right hand edge of the specimen since the tearing had tended to initiate at this end when the welding arc moved from left to right.

Since the weld metal was over-matching, the plastic strain due to external restraint was largely confined

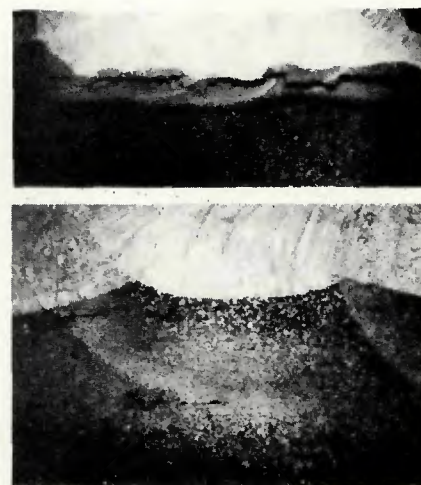


Fig. 4—Location of tears at low and high heat-input levels in semi-killed A-285 (M) steel. Top (a)—30 kJ/in. (1181 kJ/m), X6; bottom (b)—90 kJ/in. (3544 kJ/m), X14 (reduced 40% on reproduction)

to the test plate. Joint displacement reflected the strain required to cause fracture in the test plate. The load vs. displacement curve was plotted on a two-pen X-Y chart recorder, and the load and displacement as a function of time was recorded on a two-pen strip chart recorder.

The total displacement of the joint, d_T , was defined as the sum total of the two following forms of displacements:

1. Displacements at elevated temperature, d_{er} (during welding).
2. Displacements during room temperature loading between weld passes

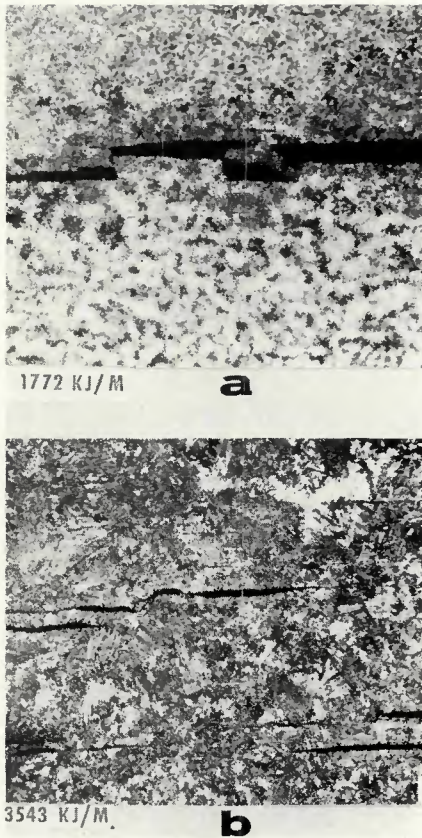


Fig. 5—Nature of subcritical tears at (a) low and (b) high heat input in semi-killed A-285 steel. 100 $\mu\text{m}/0.4375$ in. (11.1 mm) (reduced 50% on reproduction)

and following welding—Fig. 7. The free movement of the joint during welding which would result

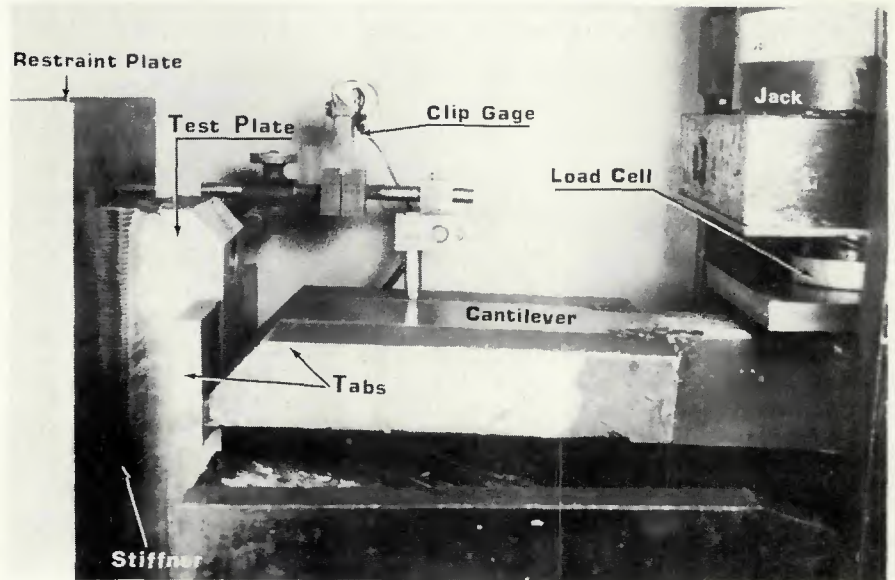


Fig. 6—Lehigh test fixture with arrangements for recording the load and joint displacement

from the thermal and transformation strains of the weldment area are opposed by the restraint imposed on the joint. The result is that the weld region must adjust by plastic strain to accommodate to the restraint. If this plastic strain induces incipient tearing (or embrittlement mechanisms), damage to the joint ductility results.

Damage due to restraint can be assessed by welding two specimens, one with zero external load and the other with a high (but subcritical) load. The two specimens can then be loaded to failure and their ductility or energy absorption compared to eval-

uate the damage caused by the restraint. Hence, a postweld energy index (E_F), the product of fracture stress (σ_F) and the displacement required to cause failure after fabrication (d_F), was calculated for each test. It was felt that this index could be used for evaluating the tearing susceptibility under different tearing welding conditions.

A series of tests were conducted on 32 mm thick semi-killed A-285 at two restraint levels to study the effect of restraint on the parameters mentioned above. To check if the behavior varied with the type of steel, two other

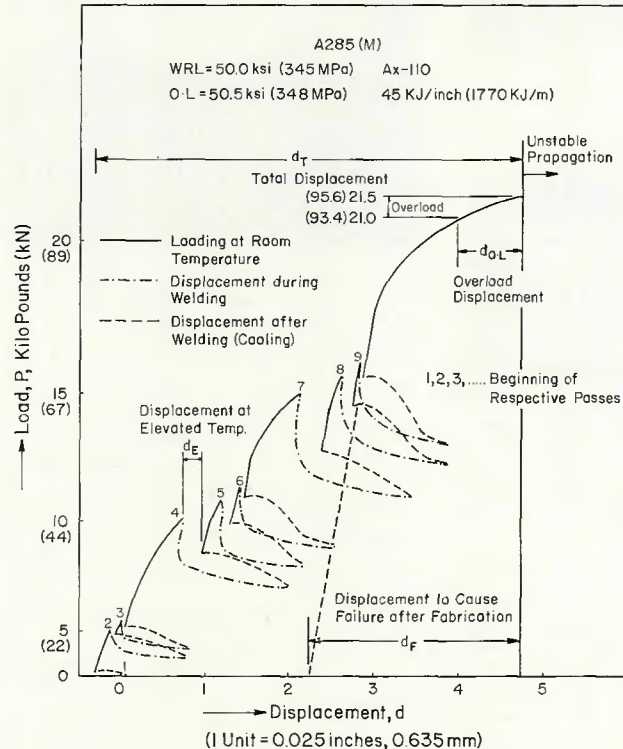


Fig. 7—Load vs. displacement curve at high restraint (as recorded)

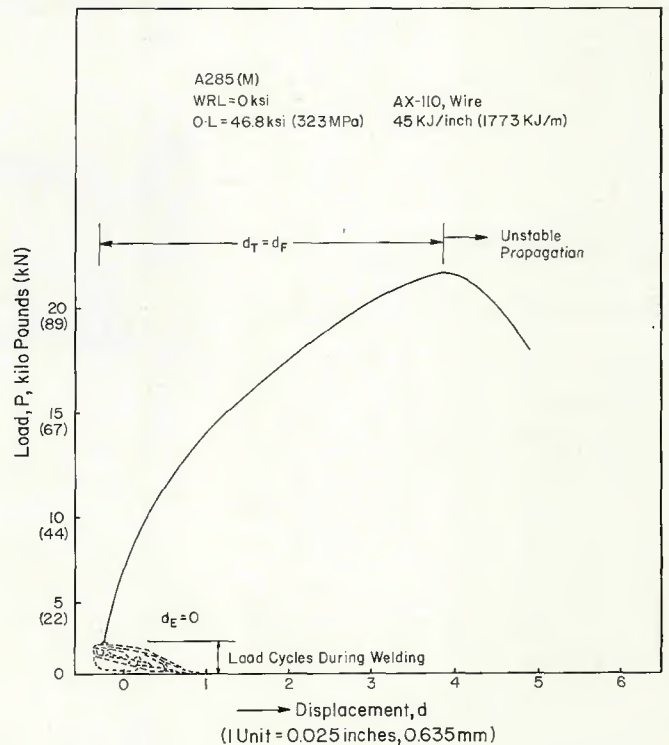


Fig. 8—Load vs. displacement curve at zero restraint (external)

steels—one 25 mm thick Si-killed (A-515-70) and one 25 mm thick Al-killed (Mil 24113C)—were included in the study of the effect of restraint level. Heat input levels of 45 kJ/in. (18 kJ/cm) (9 passes) and 160 kJ/in. (63 kJ/cm) (3 passes) were used, and the interpass temperature was maintained at room temperature. The effect of 120 C (248 F) preheat and interpass temperature was studied at the high heat input level.

These extreme conditions were chosen to maximize the comparative changes in the tearing susceptibility among the different steels. Welding was performed under two restraint levels, at low restraint (WRL = 0) and at high restraint (WRL = 50 ksi) (345 MPa) to determine the sensitivity of the steels to tearing under a fixed restraint during welding. The fracture stress (σ_F), the displacement to cause failure after welding (d_F) and the post-weld energy index (E_F) were measured

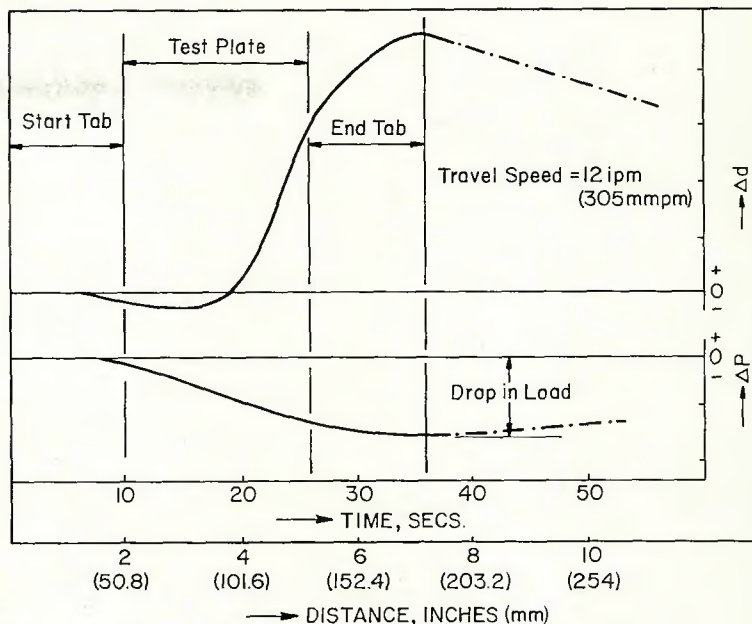


Fig. 9—Time vs. load, displacement curve

Table 6—Test Results Using the Energy Criterion

Part I

Material	Welding condition	Specimen no.	WRL,		Failure during welding	Fracture Stress σ_F		Energy index E_F	
			ksi	(MPa)		ksi	(MPa)	lb/in.	(kJ/m)
A-285(M) 1½ in. (38 mm) semi-killed	45 kJ/in. (1772 kJ/m)	8MD1	52	(359)	Yes	—	—	—	—
		8MD2	50	(345)	No	50.5	(348)	1530	(2683)
		8MD3	40	(276)	No	52.3	(361)	1621	(2834)
		8MD4	25	(172)	No	49.4	(341)	1872	(328)
		8MD5	0	0	No	46.8	(323)	2195	(384)
	45 kJ/in. (1772 kJ/m) R.D. along plate width	9MD1	50	(345)	Yes	49.0	(338)	808	(142)
		9MD2	0	0	No	53.5	(369)	2557	(447)
	45 kJ/in. (1772 kJ/m) Alternate weld direction	8MI1	50	(345)	No	56.0	(386)	2408	(421)
		8MI2	64	(441)	Yes	60.5	(418)	2118	(371)
		8ML1	48	(331)	Yes	—	—	—	—
	45 kJ/in. (1772 kJ/m) Hydrogen	8ML2	40	(276)	Yes	35.0	(240)	—	—
		8ML3	25	(172)	No	47.0	(324)	2444	(428)
		8MJ1	48	(331)	No	52	(359)	1768	(309)
		8MJ2	0	0	No	47	(324)	2444	(428)
	160 kJ/in. (6300 kJ/m) + Preheat 120 C	8MK1	50	(345)	No	57	(393)	2736	(479)
		8MK2	0	0	No	50.5	(348)	2778	(486)
8MK3		60	(414)	No	64.5	(445)	3032	(531)	
8MK4		65	(448)	Yes	63.0	(43.4)	2646	(463)	
A515-70 (F) 1 in. (25.4 mm) Si-killed	45 kJ/in. (1772 kJ/m)	8FD1	50	(345)	No	59.1	(407)	2334	(408)
		8FD2	0	0	No	48.5	(334)	1698	(297)
	160 kJ/in. (6300 kJ/m)	8FJ1	50	(345)	No	61	(421)	2684	(470)
		8FJ2	0	0	No	57	(393)	2850	(499)
		8FJ3	50	(345)	No	60	(414)	4560	(798)
		8FK2	50	(345)	No	65	(448)	5135	(894)
120 C Preheat	8FK2	65	(448)	No	68	(469)	5359	(939)	
	8UK1	50	(345)	No	57	(393)	3420	(599)	
Mil 24113C(U) 1 in. (25.4 mm) Al-killed	45 kJ/in. (1772 kJ/m)	8UD1	52	(359)	No	58.6	(404)	2256	(395)
		8UD2	0	0	No	51.8	(357)	2046	(358)
	160 kJ/in. (6300 kJ/m)	8UI1	50	(345)	No	59	(407)	3422	(599)
		8UI2	54	(372)	No	55	(379)	2310	(404)
		8UI3	0	0	No	54	(372)	3078	(539)
		8UK2	56	(386)	Yes	48	(331)	2016	(353)
		8UK3	60	(414)	Yes	59.5	(410)	3570	(625)
		8UK4	50	(345)	No	56.0	(386)	2632	(461)
120 C Preheat	8UK4	50	(345)	No	56.0	(386)	2632	(461)	

(Continued on next page)

for each test.

The effect of hydrogen was studied by passing the shielding gas through a series of water bottles to add about 1% H₂O. The welding conditions employed were identical to those used under standard conditions (i.e., 45 kJ/in. and 9 passes). The A-285 steel did not form martensite in the HAZ under these conditions of weld thermal cycling. With the high strength, low alloy filler metal (AX110), failure occurred in the weld metal, demonstrating that the weld was more susceptible to hydrogen embrittlement than the base metal. In the subsequent tests, therefore, a low strength mild steel filler metal (A-675) was used and failure then occurred by lamellar tearing in the test plate. The nature and extent of sub-critical tears

were metallographically examined by testing the specimens at a high restraint and then unloading them prior to failure.

Results

The as-recorded load-displacement curves for the A-285 plate are reproduced in Fig. 7 and 8. As the time vs. load and displacement curves were similar for all the passes, a general form of these curves is shown in Fig. 9.

In the T-joint restrained against distortion, the following events were found to occur during welding—Fig. 9:

1. At the start of welding, a slight contraction was observed without any visible change in the load. This effect

could be due to the expansion of the joint in the "start" (left hand) side which induced a slight rotational movement at the "finish" (right hand) side where the clip gage was located.

2. As welding progressed midway through the test plate, the load began to drop appreciably, accompanied by an expansion. This expansion was the sum total of thermal expansion due to welding heat and the plastic yielding of the test plate and the weldment.

3. The peak in expansion and the minimum in load occurred a few seconds after the molten puddle left the junction of the test plate and end tab.

4. After welding was stopped, the load increased steadily accompanied by contraction due to cooling of the joint.

Table 6—Test Results Using the Energy Criterion (Continued)

Part II

Material	Specimen No.	Displacement			Σ d _e (μm)	Remarks		
		d _F (μm)	D _{0L} (μm)					
A-285(M)	8MD1	—	—	—	—	Failed while loading after 7th pass		
1½ in. (38 mm) semi-killed	8MD2	30.3	(780)	8.3	(211)	11.0	(279)	—
	8MD3	31.0	(787)	18.8	(478)	10.4	(264)	—
	8MD4	37.9	(963)	30.8	(782)	5.0	(127)	—
	8MD5	46.9	(1191)	46.9	(1191)	0	0	—
	9MD1	16.5	(425)	—	—	14.7	(373)	Failed while loading after 9th pass
	9MD2	47.8	(1214)	45.9	(1166)	0	0	—
	8MI1	43.0	(1092)	15	(381)	9.9	(251)	—
	8MI2	35.0	(889)	—	—	14.3	(363)	Failed while loading after 9th pass
	8ML1	—	—	—	—	—	—	Failed while loading after 2nd pass.
	8ML2	—	—	—	—	—	—	Failed while loading after 6th pass.
	8ML3	52	(1321)	41	(1041)	0	0	Overload failure
	8MJ1	34	(864)	8.0	(203)	16.5	(419)	—
	8MJ2	52.0	(1321)	52	(1321)	0	0	—
	8MK1	48	(1219)	19.0	(483)	4.3	(109)	—
8MK2	55.0	(1397)	55.0	(1397)	0	0	—	
8MK3	47	(1194)	2.1	(53)	5.8	(147)	—	
8MK4	42	(1067)	—	—	27.5	(699)	Failed while loading after final pass.	
A-515-70(F)	8FD1	39.5	(1003)	20.2	(513)	—	—	—
1 in. (25.4 mm) Si-killed	8FD2	35.0	(889)	32.5	(826)	0	0	—
	8FJ1	44	(1118)	27.0	(686)	6.8	(173)	—
	8FJ2	50	(1270)	50.0	(1270)	0	0	—
	8FJ3	76	(1930)	43.0	(1092)	7.1	(180)	—
	8FK2	79	(2007)	47.0	(1194)	31.4	(798)	—
	8FK2	79	(2007)	9.0	(229)	17.5	(445)	—
Mil 24113C(U)	8UD1	38.5	(978)	14.0	(256)	—	—	—
1 in. (25.4 mm) Al-killed	8UD2	39.5	(1003)	39.2	(996)	0	0	—
	8UI1	58	(1473)	31	(787)	31.5	(800)	—
	8UI2	42	(1067)	4	(102)	28.6	(726)	—
	8UI3	57	(1448)	57	(1448)	0	0	—
	8UK1	60	(1524)	35	(889)	30.0	(762)	—
	8UK2	42	(1067)	—	—	44.0	(1118)	Failed while loading after final pass.
	8UK3	60	(1524)	—	—	30.0	(762)	Failed while loading after final pass.
	8UK4	47	(1194)	—	—	17.5	(450)	—

The data obtained on the three steels (A-285, A-515-70 and Mil 24113C) under different welding conditions are shown in Table 6 and graphically illustrated in Fig. 10, from which it can be seen that:

1. When 50 ksi restraint was imposed during welding the fracture stress (σ_F) increased slightly for all the three steels. Also, the joint displacement (d_F) and energy index (E_F) showed a significant drop for A-285C

and little change for A-515-70 and Mil 24113C.

2. With an increase in heat input, A-285C and A-515-70 showed a small increase in fracture stress, whereas Mil 24113C showed little change. Also, all steels exhibited a significant increase in the displacement and energy index; in Mil 24113C it was 53%, in A-285C, 15%, and in A-515-70, 20%.

3. With preheat, A-515-70 and A-285C showed a significant improve-

ment in the energy index—88% and 55% respectively. On the other hand, Mil 24113C showed practically no change. Here, it should be pointed out as significant that Mil 24113C exhibited ductile fracture at room temperature, whereas A-515-70 and A-285C were brittle.

4. With combined heat input and preheat, CWRL increased by 25% for A-285C and decreased by 6% in Mil 24113C; the energy index increased by

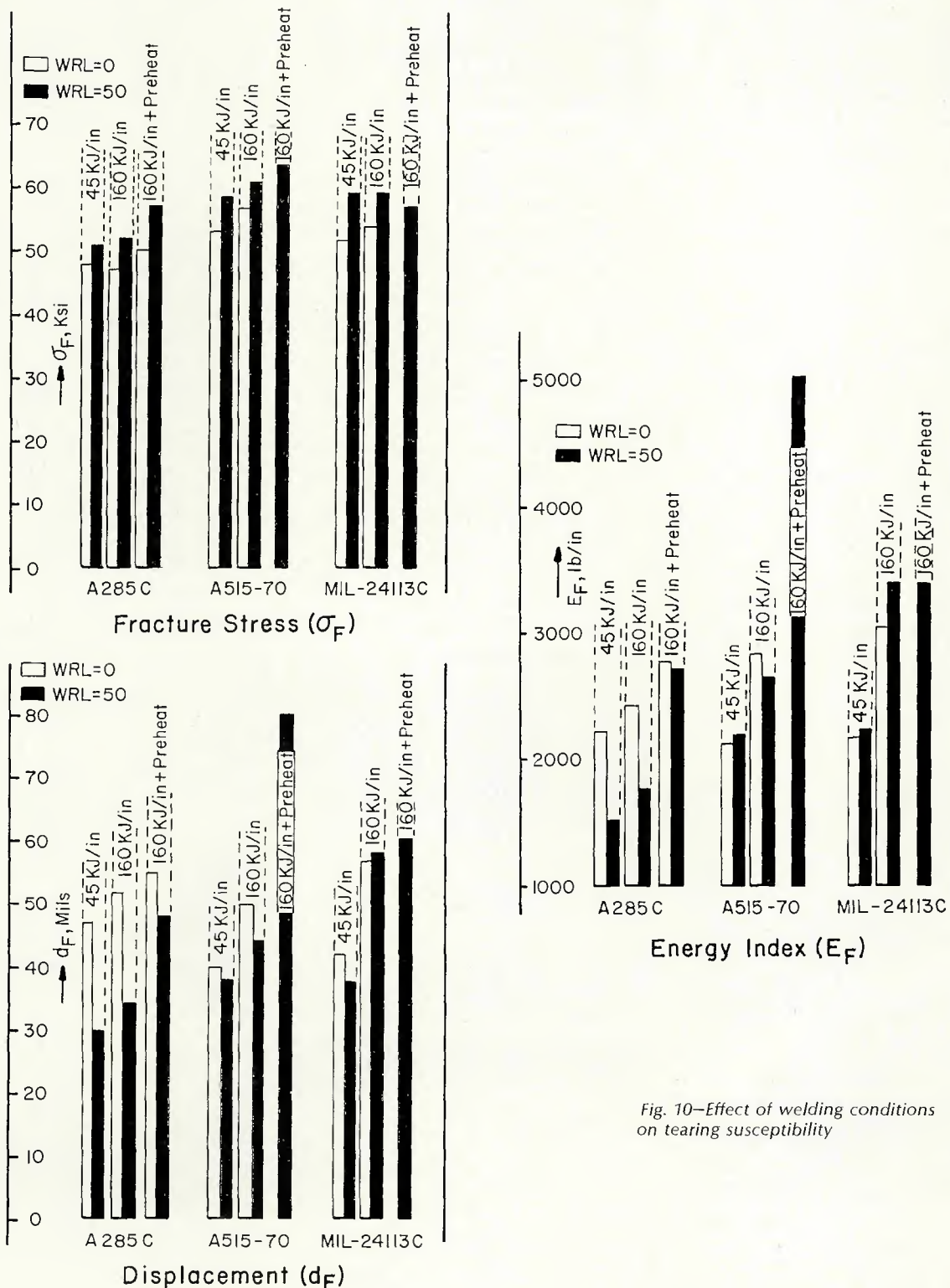


Fig. 10—Effect of welding conditions on tearing susceptibility

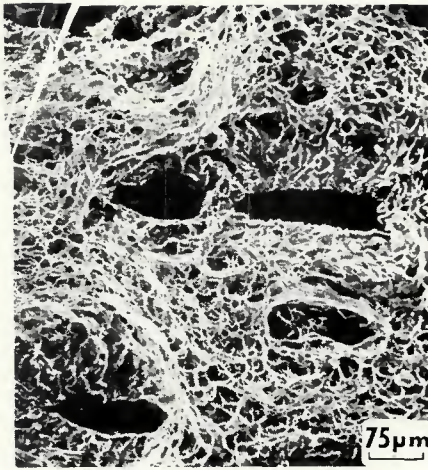


Fig. 11—Terrace fracture in semi-killed A-285 steel in the presence of hydrogen. Note the quasi-cleavage facets around the voids and microvoids in the intervening region

130% in A-515-70, 80% in A-285C and 53% in Mil 24113C.

5. With alternate welding direction, the energy index, displacement and fracture stress showed an increase of 57%, 43% and 10% respectively, in semi-killed A-285 steel; the tearing initiated at the right hand edge in one specimen and at the left hand edge in another specimen.

6. With hydrogen, the tearing resistance showed a significant decrease and the critical weld restraint level fell from 53 ksi (365 MPa) under standard conditions to about 35 ksi (241 MPa) in the presence of hydrogen; the extent of tearing, as indicated by the oxidized area on the fracture surface, was greater in the hydrogen tests than in the standard tests. In addition, the fracture surface showed the typical step-like pattern with the terraces containing elongated inclusion voids interspersed with micro-

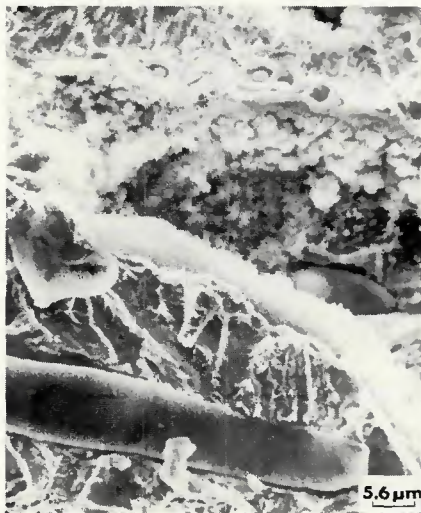


Fig. 13—White crusty deposit around inclusion void in the presence of hydrogen. Also note quasi-cleavage facets around the inclusion void at bottom

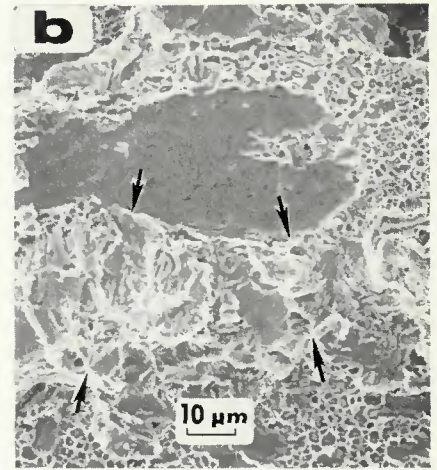
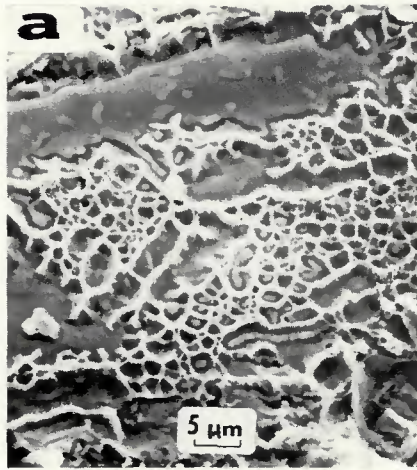


Fig. 12—Terrace fracture features in semi-killed A-285: Left (a)—without hydrogen; right (b)—with hydrogen where region between arrows shows quasi-cleavage features

voids containing smaller oxides and sulfides (Fig. 11). Moreover, the density of microvoids, the extent of void growth and the amount of quasi-cleavage facets around the voids were visibly greater in the hydrogen tests—Fig. 12. Also, areas around some inclusion voids displayed a white deposit, perhaps an hydroxide—Fig. 13.

Metallographic examination of subcritical tears revealed the following features (Fig. 14):

1. As a result of the deep penetration of the high heat input welds, tears adjacent to the first layer were interrupted and blunted by the penetrating weldment in the second layer. This phenomenon was not observed in the

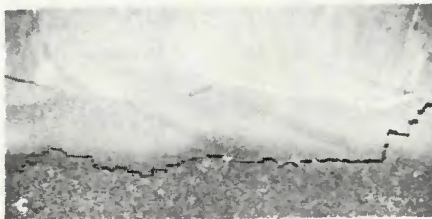
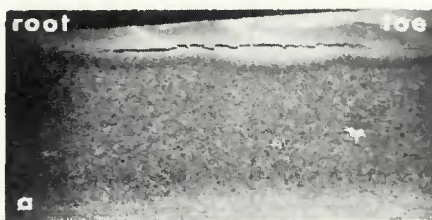
low heat input welds.

2. At high heat input, tears were confined to the HAZ in all the three steels and lay mostly in the coarse grained region. On the other hand, at low heat inputs the tears lay in the lower part of the HAZ or the unaffected base metal.

3. At high heat input, an array of terrace tears was often found ahead of the main crack and inclusion decoherence was found at several levels in the HAZ.

The fracture surface of the test specimens showed a small oxidized area in the zone of tear initiation. This was, apparently, due to the oxidation of subcritical tears formed during the

45 KJ/in



160 KJ/in; 120°C Preheat

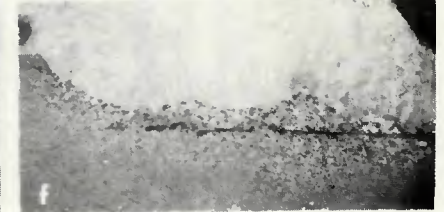


Fig. 14—Nature and location of lamellar tears at low and high heat inputs in: Top (a, b)—semi-killed A-285 (M); center (c, d)—silicon-killed A-505-70(F); bottom (e, f)—aluminum-killed Mil 24113C (U)

preceding weld passes by the heat from the overlying passes. The oxidized area was found to increase with an increase in the restraint level, heat input and preheat, suggesting increased levels of lamellar tearing during welding.

Discussion

The location of lamellar tears and the time and temperature of their formation depend on the complex interaction of weld thermal and strain cycles controlled in turn by the nature of the joint and the welding conditions employed. In a multi-pass joint, the stress-strain distribution as well as the microstructure exhibit significant local variation and tearing tends to occur when, and wherever, the local plastic strain exceeds the local ductility.

In the absence of external loading, lamellar tears did not form during welding and overload failure initiated at the toe. Thus, the results at low restraint level (WRL = 0) can be used as the base condition and compared to those at the high restraint level to estimate the degree of damage (i.e., susceptibility) due to lamellar tearing.

The minor change in the ductility and energy for the fully-killed steels when welded under high restraint suggests an absence of damage to these steels. For the semi-killed steel the significant drop in energy and ductility caused by the restraint during welding suggests incipient lamellar tearing and perhaps strain aging.

The improvement in the postweld energy index at high heat input may be due to the following factors:

1. Deeper weld penetration causing interception and arrest of pre-existing tears.
2. Reduction in the number of passes and, hence, fewer cycles for tear initiation during welding.
3. Greater relaxation of residual stresses due to slower cooling rate.
4. Softer and tougher HAZ.

With preheat, in addition to the effects mentioned above, the tearing may be retarded because of increased ductility at these temperatures. But, in actual joints preheat may enhance tearing, as reported by some investigators (Refs. 6, 7), if preheating is done in such a way as to exacerbate the contraction strains induced in the joint.

In the Lehigh test with an increase in heat input and preheat, the greater overload in the end portion of the weld, due to a larger molten puddle,

may have produced some increased lamellar tearing during welding, as evident from the larger oxidized area at the tear initiation site. However, this damaging effect was evidently off-set by the improvement resulting from crack arrest and slower cooling rates. These effects may not occur in a field-welded joint where the weld-thermo mechanics are likely to be different from the situation in the Lehigh test. Ganesh (Ref. 12) has proposed some modifications to the test to simulate more closely the situation in an actual joint.

Some investigators have attributed the detrimental effect of hydrogen to an increase in the local hydrogen concentration at the inclusions due to the pile up of hydrogen-carrying dislocations against them. The excess hydrogen causes a reduction in the interfacial strength, stabilization of the voids and enhanced void growth due to internal pressure.

Beachem (Ref. 13) has suggested a model by which hydrogen dissolved in the lattice ahead of the crack tip acts to localize the crack tip deformation by whatever mode the matrix favors, rather than to embrittle the lattice by inhibiting deformation. The fracture mode tends to progress from intergranular to quasi-cleavage to microvoid coalescence with an increase in the stress intensity or hydrogen concentration at the crack tip. Thus, in the early steps of tearing when the crack length and, hence, the stress intensity is small, fracture around inclusion voids tends to occur by quasi-cleavage (in HAZ)—and in the later steps, when the stress intensity is higher, by microvoid coalescence. This was confirmed by frequent observation of quasi-cleavage features around the large inclusion voids, which apparently formed first, and microvoids in the intervening region.

Summary

In the Lehigh test, the postweld energy index was found to disclose some additional aspects of lamellar tearing susceptibility that are not indicated by the critical weld restraint level. In particular, there is an increase in postweld ductility produced by higher heat inputs or by preheat that is revealed by the energy index.

While the extent of subcritical tearing, as seen on the fracture surface, increased with an increase in heat input and preheat, susceptibility to failure, as indicated by the post-weld energy index, decreased. Interception

and blunting of tears adjacent to the toe of the preceding weld layer was observed to result from the finger penetration of the overlying weld.

Alternating the welding direction after each pass led to significant decrease in the initiation of lamellar tearing.

The presence of hydrogen in the arc atmosphere significantly lowered the tearing resistance of the A-285 steel even in the absence of a martensitic heat-affected zone. Fracture occurred by a combination of quasi-cleavage and microvoid coalescence.

References

1. Oates, R. P. and Stout, R. D., "A Quantitative Weldability Test for Susceptibility to Lamellar Tearing," *Welding Journal*, 52 (11), Nov. 1973, Research Suppl., 481-s to 491-s.
2. Jubb, J. E. M., Currick, L. and Hammond, J., "Some Variables in Lamellar Tearing," *Metal Construction and British Welding Journal*, Vol. 1, No. 2, Feb. 1969, pp. 58-63.
3. Nicholls, D. M., "Lamellar Tearing in Hot Rolled Steel," *British Welding Journal*, Vol. 15, No. 3, March 1968, pp. 103-112.
4. Araki, M., et al., "Cracking in Multirun Fillet Welds," *Nippon Kokan Technical Report-overseas*, June 1974, pp. 25-35.
5. Amemya, Y., Satake, M., Kajimoto, K. and Ohba, K., "Effects of Welding Procedure and Steel Materials on Prevention of Lamellar Tearing," *International Institute of Welding*, Doc. No. IX-780-72, May 1972.
6. Lombardini, J., "Cracking as a Criteria for Weldability," *Metal Construction and British Welding Journal*, Vol. 1, No. 2, Feb. 1969, pp. 40-43.
7. Farrar, J. C. M. and Dolby, R. E., "An Investigation into Lamellar Tearing," *Metal Construction and British Welding Journal*, Vol. 1, No. 2, Feb. 1969, pp. 32-34.
8. "Discussion on Lamellar Tearing," *Metal Construction and British Welding Journal*, Vol. 1, No. 2, Feb. 1969, pp. 117-124.
9. Nishio, Y., Yamamoto, Y., Kajimoto, K. and Hirozane, T., "On Lamellar Tearing in Multirun Fillet Welds," *Technical Review*, Vol. 9, No. 3, Oct. 1972, Mitsubishi Heavy Industries Ltd., Japan.
10. Arita, Y. and Kajimoto, K., "The Study of Lamellar Tearing in Offshore Structure," *Fourth Annual Offshore Technology Conference in Houston, Texas*, May 1972.
11. Ganesh, S., and Stout, R. D., "Material Variables Affecting Lamellar Tearing Susceptibility in Steels," *Welding Journal*, 55 (11), Nov. 1976, Research Suppl., 341-s to 355-s.
12. Ganesh, S., "Study of Variables Affecting Lamellar Tearing Susceptibility," Ph.D. Dissertation, Lehigh University, Bethlehem, Pa., May 1976.
13. Beachem, C. D., "A New Model for Hydrogen-assisted Cracking (Hydrogen "Embrittlement")," *Met. Transactions*, Vol. 3, February 1972, pp. 437-451.